

**Buckling test of stiffened panels
Modeling and vibrational correlation testing**

Peeters, D.M.J.; Pagani, Alfonso; Augello, Riccardo; Carrera, Erasmo; do Prado, Alex Pereira; Cabral, Pedro Higinio; dos Santos, Henrique E.A.A.

Publication date
2022

Document Version
Final published version

Published in
Proceedings of the 20th European Conference on Composite Materials: Composites Meet Sustainability

Citation (APA)

Peeters, D. M. J., Pagani, A., Augello, R., Carrera, E., do Prado, A. P., Cabral, P. H., & dos Santos, H. E. A. (2022). Buckling test of stiffened panels: Modeling and vibrational correlation testing . In A. P. Vassilopoulos , & V. Michaud (Eds.), *Proceedings of the 20th European Conference on Composite Materials: Composites Meet Sustainability: Vol 4 – Modeling and Prediction* (pp. 763-770). EPFL Lausanne, Composite Construction Laboratory.

Important note

To cite this publication, please use the final published version (if applicable).
Please check the document version above.

Copyright

Other than for strictly personal use, it is not permitted to download, forward or distribute the text or part of it, without the consent of the author(s) and/or copyright holder(s), unless the work is under an open content license such as Creative Commons.

Takedown policy

Please contact us and provide details if you believe this document breaches copyrights.
We will remove access to the work immediately and investigate your claim.

BUCKLING TEST OF STIFFENED PANELS: MODELING AND VIBRATIONAL CORRELATION TESTING

Daniël, Peeters^a, Alfonso, Pagani^b, Riccardo, Augello^b, Erasmo, Carrera^b, Alex, Pereira do Prado^c, Pedro, Higino Cabral^c, Henrique, Dos Santos^d

a: Delft University of Technology, faculty of Aerospace Engineering, section: Aerospace Structures and Computational Mechanics – d.m.j.peeters@tudelft.nl

b: MUL2, Department of Mechanical and Aerospace Engineering, Politecnico di Torino, Torino, Italy

c: Embraer S.A., São José dos Campos, Brazil

d: Instituto Tecnológico de Aeronautica, São José dos Campos, Brazil

Abstract: *Representative stiffened panels are optimized such that multiple buckling modes and failure (using open hole allowables) occur within a range of 10% of the lowest buckling load. This implies the panels cannot be loaded up to the buckling load without risking failure, hence vibrational correlation testing was used to estimate the buckling loads and modes. At the same time, a finite element model was created using the Carrera Unified Formulation. This model was validated using the tests and a good correlation between both was observed. Three panels were manufactured and each panel was put in place for testing twice. Each time a panel was put in place, the test was repeated three times. This allowed us to get a ballpark estimate for the variation due to replicas of the panel, the test set-up and repeating the tests.*

Keywords: vibrational correlation; buckling; stiffened panel

1. Introduction

The uncertainty or spread in properties is usually checked at the coupon level in terms of the material properties. However, it is not the spread in the material properties, but the spread of the performance of the resulting structure that is of interest to the user. In this work, the buckling load of a panel will be investigated using Vibration Correlation Testing (VCT). The outcome will lead to insights in the cause of the scatter, besides material scatter which is already studied more frequently.

The key assumption of VCT is that the vibration modes are similar to the buckling modes. By using that assumption, one can plot the relationship between the natural frequencies and the progressively higher applied (compression) loading. By extrapolating this relationship, the buckling load can be estimated as the load where the natural frequency is zero [1]. The advantage of VCT is that the buckling load can be estimated without the need to buckle the structure, which may lead to panel failure.

In the ideal case of stable buckling (i.e., Euler buckling), the natural frequency squared and the compressive load are linearly dependent [2], so that:

$$\left(\frac{f}{f_0}\right)^2 + \left(\frac{P}{P_{cr}}\right) = 1 \quad (1)$$

where f is the natural frequency of the structure under load P , f_0 is the natural frequency of the unloaded structure, and P_{cr} is the critical buckling load. In [3] it was shown that eq. (1) works

well for simply supported columns, but for other types of structures or boundary conditions, the curve becomes curved rather than the straight line predicted by eq. (1). One of the more advanced formulations reads [4,5]

$$\left(1 - \frac{P}{P_{cr}}\right)^2 + (1 - \xi^2) \left(1 - \left(\frac{f}{f_0}\right)^4\right) = 1 \quad (2)$$

where ξ represents the experimental knock-down factor. In the present work, the VCT method used is similar to eq. (2).

In this work, we aim to investigate the influence of different parts (called replica's in the current work), the influence of the test set-up and the repetition of the same test with the same test set-up. For this purpose three stiffened panels are manufactured. The tests done are compression test where VCT is used to assess the panel's response and estimate the buckling load and buckling mode. This type of test allows us to accurately estimate the buckling load, without risking to break the panel.

2. Design and manufacturing

2.1 Design and analysis

The panels were optimized using the slice and swap method [6] in terms of lamination parameters, in such a way that multiple buckling modes happen within 10% of the lowest buckling load. Furthermore, failure of the panel (using open-hole allowables) also happened in this load region. Next to the lamination parameters also the width, height and thickness of the stiffener and the thickness of the panel were changed during the optimization. The 50 mm on each side (which in reality is encapsulated in a resin block), shown on the left in Figure 1, is not taken into account in this optimization, instead a simply supported line load is used.

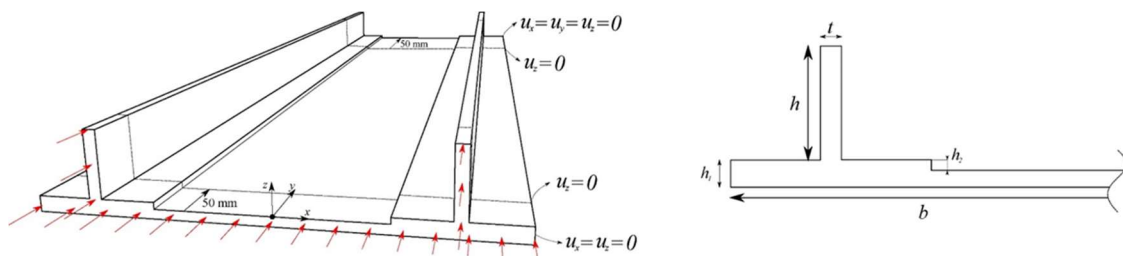


Figure 1. Panel dimensions (left) and stiffener dimensions (right)

The end result of the optimization is a two-stringer reinforced panel with a length of 690 mm (free length) and width b of 270 mm. On the right of Figure 1 the dimensions of the final cross-section are shown. Here, the stringer height and thickness are $h = 39.3$ mm and $t = 7.3$ mm, respectively, whereas $h_1 = 9.52$ mm and $h_2 = 3.66$ mm. Afterwards, the design is transferred into a stacking sequence using 0/90/45/-45 degree plies. Since failure and buckling happen so close together, the VCT method is used to estimate the buckling load to allow multiple repetitions of the test without risk of braking the panel.

After design, more detailed analysis of the panel is performed, including the 50 mm resin blocks that are used on the outside. This detailed analysis is performed using the Carrera Unified Formulation (CUF) [7]. The main advantage of this method is that classical to higher-order models can be implemented with ease in an automated way. In fact, the governing equations

and the related finite element arrays are written in terms of theory-independent fundamental nuclei (kernels) in CUF. When extended to laminated composite structures, it is therefore possible to formulate advanced models with layer-wise kinematics [8]. CUF-based layerwise models are computationally efficient and provide accurate through-the-thickness stress states [9], which are of fundamental importance in the nonlinear analysis and whenever a rigorous estimation of the tangent (incremental) stiffness is required, such as in the case of VCT simulations. The buckling modes predicted are shown in Figure 2.

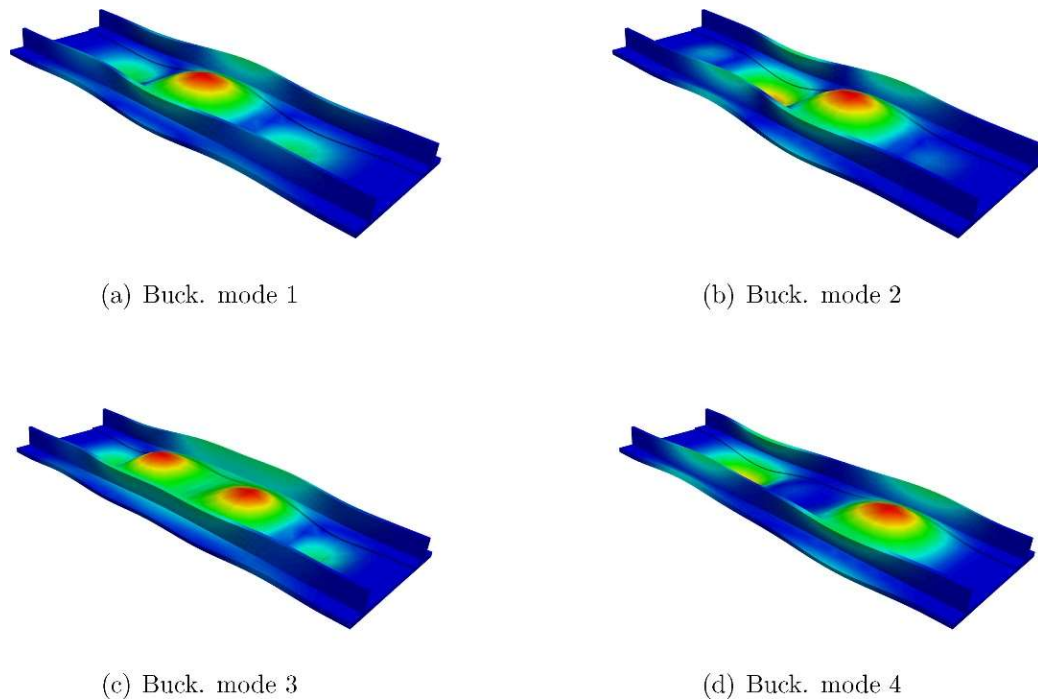


Figure 2. buckling modes from finite element simulations

2.2 Manufacturing

The reinforced composite panels were manufactured at the Delft Aerospace Structures and Materials Laboratory. The AS4 unidirectional prepreg employed has the following material properties: $E_1=119$ GPa, $E_2=9.8$ GPa, $E_3=4.67$ GPa, $\nu_{12}=0.316$, $\nu_{13}=0.026$, $\nu_{23}=0.33$, $G_{12}=4.7$ GPa, $G_{13}=G_{23}=1.76$ GPa, and $\rho=1580$ kg/m³. Note that the properties in the out-of-plane directions (13 and 23) are assumed and not available from the manufacturer.

As a first step, the layers of the skin were stacked on top of each other, regularly debulking to ensure good bonding between the layers. The stiffeners were manufactured by making two parts from the same layup, again often debulking them. One of the two parts was flipped before being bent in L format to guarantee that the stringer web was symmetric, and finally the two L-parts were put back-to-back, obtaining the T-stringer. The noodle at the bottom between the two L-parts was filled up using unidirectional 0 degree material. Finally, the stiffeners were carefully placed on the panel and the stiffened composite panel was co-cured as a whole. During curing, care was taken to ensure that the pressure was evenly distributed, the stiffeners did not fall over and stayed in their intended position on the panel.

After curing, all sides of the panel were trimmed to their final dimensions. To provide the clamped boundary conditions on the short edges, the outer 50 mm were molded in an epoxy.

This epoxy was flattened to ensure the compression load is applied perfectly in line with the panel. The final dimension of the panel used for the simulation is the ‘free’ length: the part molded in the epoxy is not modeled. The three finished panels are shown in Figure 3.



Figure 3. Manufactured panels

3. Testing

3.1 Test plan

Since the main goal is to get a grip on the source of variation, we have used a nested or hierarchical design of experiments [10]. In our case there are two levels we want to investigate: the influence of replica’s and the test set-up, and both may have an influence on the result. We have set up three replica’s, and each replica will be put in the test set-up twice in a random order. For each set-up, three measurements are performed to check the influence of the measurement accuracy. A graphical representation of the test plan can be seen in Figure 4.

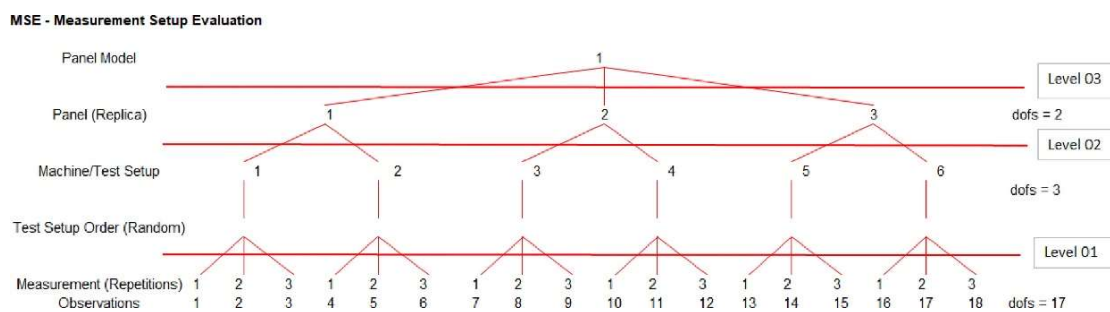


Figure 4. Test plan

3.2 Test preparation

The compression tests were performed using a MTS machine with a maximum force of 3500 kN and an accuracy of 1 kN. One of the panels placed in this machine is shown in Figure 5. During the compressive loading, VCT was performed with loads up to 600 kN; i.e. approximately 80% of the expected buckling load. A Polytec laser vibrometer was used for the data acquisition. A shaker was used as excitation device, using a frequency sweep between 0 and 1000 Hz. The load was gradually changed to ensure the panel does not fail due to dynamic defects. A measurement

with the vibrometer was performed every 100 kN, leading to six measurements. The shortening was measured using two linear vertical displacement transducers (LVDT): one was placed on each side of the panel to ensure the panel was loaded in pure compression and no moment was induced on it. The test set-up is shown in Figure 5.

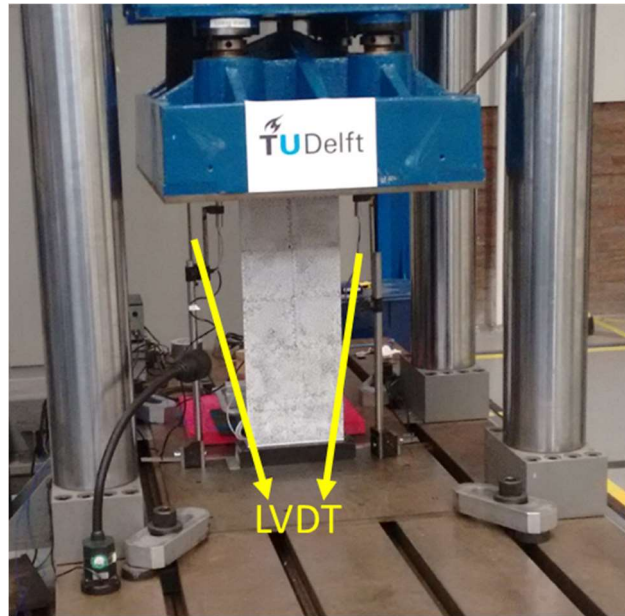


Figure 5. Test set-up

The VCT was performed using a 7x3 mesh, which allows to track the expected buckling modes. During the test the first four frequency response function peaks were tracked. By tracking the mode shapes, we can determine the frequency change at each loading level. This information is then extrapolated to predict the linear static buckling load (i.e., the location with zero frequency) in a nondestructive way, reducing the chance of introducing defects in the panel during the repeated loading tests.

4. Results and discussion

Before diving into the VCT result and buckling, first the stiffness in compression of the panels is checked, by comparing the E-modulus of the different panels with the finite element models. The Nastran model was built by using 2D CQUAD elements, based on a first-order shear approximation theory and homogenized properties across the thickness. The results are shown in Table 1. It can be seen that very little scatter is present between the panels, and a good correlation with the finite element models exists. As demonstrated previously in literature, the Nastran model is appropriate for linear static considerations, but should be avoided when the evaluation of the internal stress state is of fundamental importance, for example for failure and buckling calculations.

The results of the VCT calculation for the different modes is shown in Table 2. The average of all tests is used in this table to compare to the CUF model. The Nastran model is not used for these calculations. For frequency 4, there is no data for the first measurement loads since this mode is not one of the lowest 4 modes measured at the lower loads, the frequency at these loads is unknown. In general, a good match between the experiments and the CUF model is observed. The small differences will not affect the conclusions.

Table 1: Compression test: stiffness results.

	Shortening [mm]	Loading [kN]	Compression modulus [MPa]
Panel 1	2.61	599.97	229.9
Panel 2	2.61	599.82	229.8
Panel 3	2.61	599.98	229.9
Nastran	2.41	600	249.0
CUF model	2.41	600	249.0

Table 2: Vibration analysis: comparison of CUF model and experiments.

Load [kN]	f ₁ [Hz]	f ₁ [Hz]	F ₂ [Hz]	f ₂ [Hz]	f ₃ [Hz]	f ₃ [Hz]	f ₄ [Hz]	f ₄ [Hz]
	CUF	exp.	CUF	exp.	CUF	exp.	CUF	exp.
100	349	348	462	459	550	555	622	—
200	330	339	447	457	537	553	578	—
300	308	324	431	449	523	546	532	—
400	284	304	415	436	513	535	476	514
500	258	281	398	420	499	522	414	462
600	225	253	381	407	487	505	336	394

The measured frequencies, as a function of the compression load is graphically shown in Figure 6. Here also the confidence interval of the tests is provided. On the graph on the left it can be observed that the first two buckling modes are also with the VCT method predicted to be very close together. The fourth frequency, which is only measured from 400 kN onwards, is rapidly decreasing and is the second buckling mode expected. The second and third frequency decrease slower and are linked to a much higher buckling load. On the right, the predictions with the CUF model and the extrapolated experimental data can be seen, which both lead to two buckling loads being close together, but the experiments over-estimate the buckling load.

The measured modes using VCT are shown in Figure 7. The first and fourth mode, which are expected to be the first two buckling modes based on the extrapolation, show a good match with the buckling modes expected based on the simulation. Modes 2 and 3 are related to the stiffener or outsides of the plate buckling, which does not match the expected buckling modes. This is however expected since the extrapolated load at which these modes reach a zero frequency is a lot higher than the first buckling load.

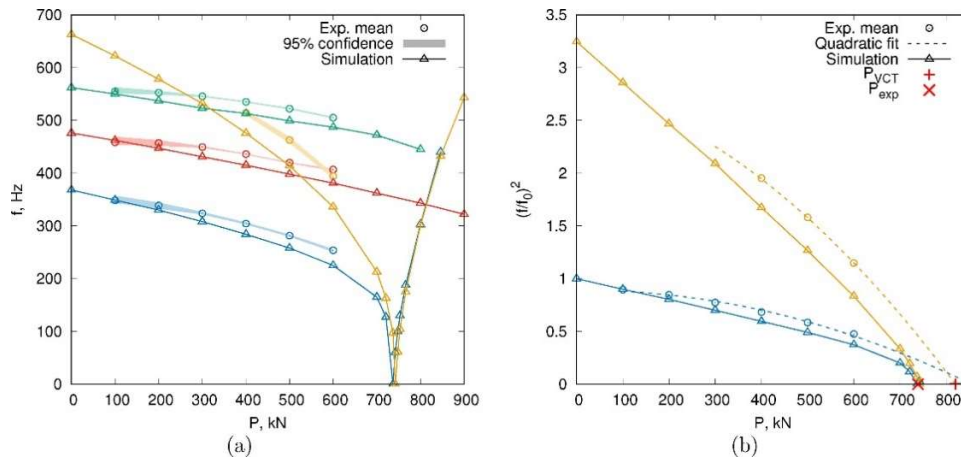


Figure 6. VCT results

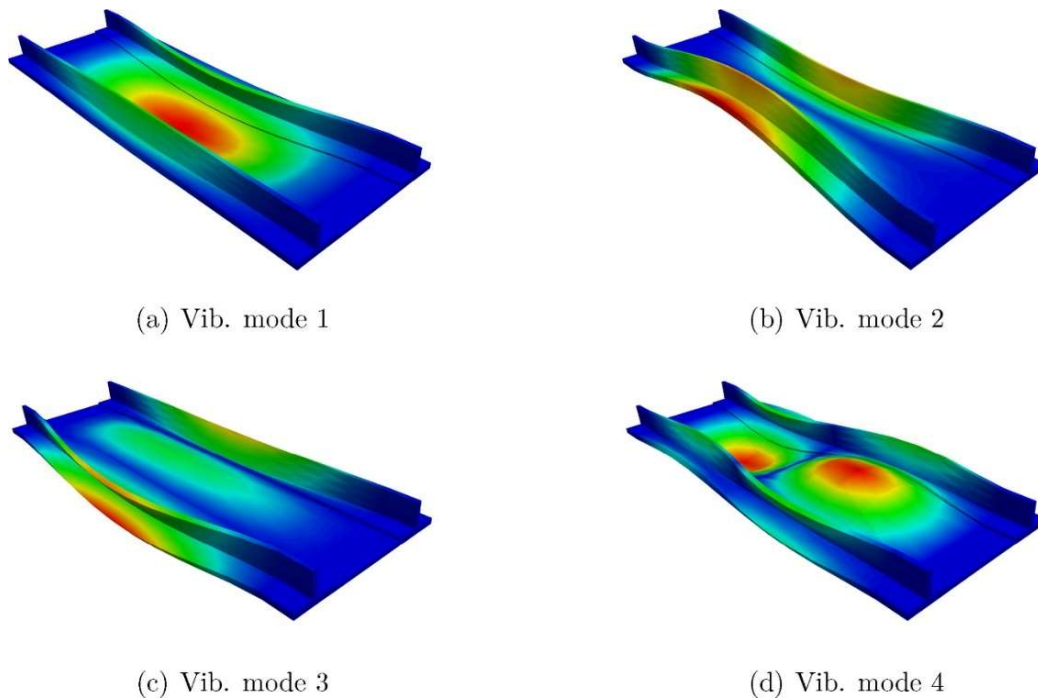


Figure 7. vibrations modes obtained from CUF model

Based on the different tests, it was found that the different set-ups could not be distinguished from each other at 200 kN since the natural variation of the measurements (i.e., repeating the same test without changing the set-up) has the same magnitude as the variance between test set-ups. This shows that the test set-ups cannot be distinguished from each other, and that the test set-up gives a very good repeatability.

5. Conclusion

The current work shows a first step towards getting a grip on the variation between structural parts and where they come from. A stiffened panel was optimized to have multiple buckling modes and failure within a margin of 10% of the lowest buckling load. Using CUF, the stiffness, buckling loads/modes and natural frequencies at different compressive loads were predicted.

The finite element results and experiments showed a good match, highlighting the potential of this method to be used during design.

The influence of the test set-up and replicas could not be distinguished in this case due to the relatively low number of tests. The results do give a ballpark figure for the variation due the replica's and the test set-up. With this information, we can expand our experimental configuration in order to improve the standard variation estimates to also include other important factors such as different material batches and/or parts suppliers, for example.

6. References

1. J. Singer, J. Arbocz, and T. Weller. Buckling experiments, shells, built-up structures, composites and additional topics, volume 2. John Wiley & Sons, 2002.
2. L.N. Virgin and R.H. Plaut, Effect of axial load on forced vibrations of beams, *Journal of Sound and Vibration*, 168(3):395-405, dec 1993
3. H. Abramovich, D. Govich, and A. Grunwald. Buckling prediction of panels using the vibration correlation technique. *Progress in Aerospace Sciences*, 78:62-73, 2015.
4. M.A. Souza, W.C. Fok, and A.C. Walker. Review of experimental techniques for thinwalled structures liable to buckling, Part I - neutral and unstable buckling. *Experimental Techniques*, 7(9):21-25, sep 1983.
5. M.A. Souza, W.C. Fok, and A.C. Walker. Review of experimental techniques for thinwalled structures liable to buckling, Part II - stable buckling. *Experimental Techniques*, 7(10):36-39, oct 1983.
6. G. H. C. Silva, A. P. do Prado, P. H. Cabral, R. De Breuker, and J. K. S. Dillinger, Tailoring of a composite regional jet wing using the slice and swap method, *J. Aircraft.*, vol. 56, no. 3, pp. 990–1004, 2019
7. E. Carrera, M. Cinefra, M. Petrolo, and E. Zappino, *Finite Element Analysis of Structures through Unified Formulation*. John Wiley & Sons, Chichester, West Sussex, UK, 2014.
8. A. Pagani, A. G. de Miguel, M. Petrolo, and E. Carrera, Analysis of laminated beams via unified formulation and Legendre polynomial expansions, *Compos. Struct.*, vol. 156, pp. 78–92, 2016
9. A. G. de Miguel, I. Kaleel, M. H. Nagaraj, A. Pagani, M. Petrolo, and E. Carrera, Accurate evaluation of failure indices of composite layered structures via various Fe models, *Compos. Sci. Technol.*, vol. 167, pp. 174–189, 2018
10. D. C. Montgomery, *Design and Analysis of Experiments*, Wiley Hoboken, NJ, 1984